A multiproxy approach to tracking aridity across Australian landscapes using brushtail possums (Marsupialia: Phalangeridae: *Trichosurus*)

By

Eva Marie Biedron

Thesis

Submitted to the Faculty of the

Graduate School of Vanderbilt University

in partial fulfillment of the requirements

for the degree of

MASTER OF SCIENCE

in

Earth and Environmental Science

August 10, 2018

Nashville, Tennessee

Approved:

Larisa R. G. DeSantis, Ph.D.

Ralf Bennartz, Ph.D.

ACKNOWLEDGMENTS

I would like to thank my advisor, Larisa R. G. DeSantis, for her expertise and endless patience, and my second reader, Ralf Bennartz, for bringing a satelite's-eye view to this project. Additionally, I would like to thank Maria Luisa Jorge, Jessica Oster, and David Furbish for reading term paper after term paper about brushtail possums; this work would not be as polished without several years of their commentary behind its varied iterations. Finally, I could not have done this without the support from the members of the Earth and Environmental Sciences Department. Finally, I would like to thank the Geological Society of America for funding this work with a Graduate Student Research Grant, as well as the National Science Foundation (Grant 1455198 to Larisa Grawe DeSantis) and Vanderbilt University for providing financial support.

TABLE OF CONTENTS

LIST OF TABLES

LIST OF FIGURES

Chapter 1

A multiproxy approach to tracking aridity across Australian landscapes using brushtail possums (Marsupialia: Phalangeridae: *Trichosurus*)

1.1 Introduction

Anthropogenic climate and habitat change is affecting vertebrates, including mammals, across the world (Maclean & Wilson, 2011). Australia, which is dominated by a highly endemic fauna and prone to extreme climatic events (Black, Archer, Hand, & Godthelp, 2012; Black, Price, Archer, & Hand, 2014), has been unduly affected— with one recent estimate suggesting that more than one–third of the worlds modern mammal extinctions are occurring there (Woinarski, Burbridge, & Harrison, 2015). Additionally, patterns of modern Australian mammal extinctions are opposite to that of other ecoregions and disproportionately affecting small mammals, even in regions where non–endemic predators are absent (Murphy & Davies, 2014). Arboreal marsupials in particular may be especially sensitive to increases in temperature in already warm tropical rainforests in Australia (Williams, Bolitho, & Fox, 2003). Climate projections indicate a 2.8 °C increase in temperature across Australia by 2050 (a similar temperature increase is projected globally by 2100), while continent–wide aridification will become more pronounced (Cleugh, Battaglia, Graham, Smith, 2011). In light of these predictions, it is critical to understand how Australia's endemic marsupial fauna may respond to current climate change.

While mammalian responses to climate change can be studied on short timescales, a deep–time perspective provided by paleontological studies can allow scientists to assess longer–term responses to climate change, such as during periods of pronounced global warming or cooling (Cerling, Harris, MacFadden, Leakey, Quade, Eisenmann, Ehleringer, 1997; DeSantis, Feranec, & MacFadden, 2009; Janis, Damuth, & Theodor, 2000; Secord *et al.*, 2012; Travoullion, Legendre, Archer, & Hand, 2009). Australia has a geological

past characterized by aridification, resulting in the decline of forests throughout the interior of the continent (*e.g.* Black *et al.*, 2014; Hocknull, Zhao, Feng, & Webb, 2007; Kershaw, Moss, & van der Kaars, 2003; Travoullion *et al.*, Legendre, Archer, & Hand, 2009). During the middle to late Miocene, Australian rainforest habitats were increasingly replaced by sclerophyll vegetation, while faunal diversity declined and surviving species became better adapted to more arid and open environments (Travoullion *et al.*, 2009). This pattern continued through the Pliocene and into the Pleistocene, where continent–wide warming and habitat change are hypothesized to have caused extinctions in both small and large marsupial mammals (Hocknull *et al.*, 2007; Kershaw *et al.*, 2003). The Australian Cenozoic paleontological record represents a natural experiment that may improve deep–time understanding of marsupial responses to habitat and climatic change.

Ice core records can aid in understanding global climate change over the past approx. 800 ka (*e.g.* Jouzel *et al.*, 2007; Kershaw *et al.*, 2003); other methods are able to assess climate archives with older and more local signals. Fossil teeth contain a treasure trove of ecological proxy information. Stable carbon and oxygen isotope analysis of tooth enamel can indicate the consumption of C_3 and/or C_4 plants by herbivores, as well as potential evaporative conditions of their local environment, respectively (Cerling *et al.*, 1997; Murphy, Bowman, & Gagan, 2007a, b; Levin, Cerling, Passey, Harris, & Ehleringer, 2006, Van der Merwe & Medina, 1991). However, in ecosystems that contain both C_3 and C_4 grasses and shrubs (like Australia), dental microwear analysis is able to distinguish the physical properties and thus, type of vegetation consumed when combined with stable isotope evidence (Prideaux, Ayliffe, DeSantis, Schubert, & Murray 2009; DeSantis, Field, Rowe, & Dodson, 2017). Proxy methods like these can unlock valuable environmental information from even small or fragmentary teeth, allowing for widespread application.

Oxygen isotopes reflect water consumed by local animals (Levin, Cerling, Passey, Harris, Ehleringer, 2006), allowing for potential reconstructions of relative aridity. Animals that predominantly drink free–standing water are termed 'evaporation insensitive' because

there are no large changes to their enamel δ^{18}O values with increased water deficits, while 'evaporation sensitive' taxa (which obtain dietary water primarily through the consumption of evaporative plant water) do demonstrate increased δ^{18}O values with increased aridity (Levin *et al.*, 2006). δ^{18}O enamel values in macropodids (*i.e.* kangaroos and their relatives) are inversely correlated with relative humidity (Murphy *et al.*, 2007a) and are also higher in warmer and/or dryer environments as compared to cooler and/or wetter environments in South Australia (Prideaux *et al.*, 2007). Additionally, vegetation and seasonal changes may be tracked using molar enamel of the genus *Macropus* (Brookman & Ambrose, 2012). Vombatid (*i.e.* wombat) oxygen isotopes can also differentiate whether the organism occupied arid to semi–arid or temperate to coastal environments in Australia (Fraser, Günn, Privat, & Gagan, 2008). Relative humidity and mean annual precipitation significantly predict δ^{18}O values in koala (*Phascolarctos cinerus*) enamel, suggesting that relative aridity can be inferred from arboreal marsupials in addition to ground dwelling kangaroos (DeSantis & Hedberg, 2017).

Carbon isotopes from tooth enamel can reveal the photosynthetic pathway of the plants consumed by herbivores, in addition to the relative density of forests occupied and/or the height at which arboreal taxa consume vegetation (Cerling *et al.*1997; Murphy*et al.*, 2007b; Prideaux *et al.*, 2009; van der Merwe & Medina, 1989; van der Merwe & Medina, 1991). For example, animals occupying more open forests and/or feeding higher in the canopy where sunlight is the greatest have higher δ^{13}C values than in more densely canopied forests and/or when feeding lower in the canopy (van der Merwe & Medina, 1989; van der Merwe & Medina, 1991; Cerling, Hart, & Hart, 2004). As C_3 plants have a mean δ^{13}C value of approx. –27‰ and C_4 plants have an mean δ^{13}C value of approx. –12‰ (Cerling *et al.*, 1997), medium– to large– size marsupial enamel values of –9 to –3‰ are reflective of a mixed C_3 and C_4 plant diet (when also considering enrichment rates of approximately 13.3‰ between the diet and enamel in kangaroos and wombats; Fraser *et al.*, 2008; Prideaux *et al.*2009). Subsequently, δ^{13}C values less than –9‰ suggest the consumption

of vegetation from dense shrubs and/or forests (based on Cerling *et al.*1997; Cerling *et al.*2004; Prideaux *et al.*2009; van der Merwe & Medina, 1989; van der Merwe & Medina, 1991).

Analysis of dental microwear can aid in differentiating between disparate diets consisting of tough or hard food items. Unlike stable carbon isotopes, dental microwear captures the textural properties of food items consumed days to weeks before an animal's death (the last supper effect; Grine, 1986). Scale-sensitive fractal analysis of high-resolution 3D elevation models of dental surfaces allow for dental microwear to be quantified and compared across populations and between different taxa (Ungar, Brown, Bergstrom, & Walkers, 2003; Scott *et al.*, 2005; Scott *et al.*, 2006; DeSantis, 2016). DMTA has been applied to several macropodids, revealing disparate dental microwear attributes between extant grazers and browsers (DeSantis *et al.*, 2017; Prideaux *et al.*, 2009). DMTA demonstrates that koalas consume tough foods (as observed) and that higher complexity values in some individuals may reflect the increased consumption of woody browse in more temperate regions (Hedberg & DeSantis, 2017). However, more work is needed to better understand if and how dental microwear textures of enamel wear facets are correlated with different diets and/or an animal's local environment including grit loads.

Before proxy methods like stable isotope analysis and DMTA can be used to investigate the environments inhabited by ancient Australian marsupials, they must be calibrated through the examination of modern relatives. Apart from work performed on koalas (DeSantis & Hedberg, 2017; Hedberg & DeSantis, 2017), little is known about how arboreal marsupials track their local climate and environment using either of these proxy methods. Considering Australia was once dominated by arboreal taxa (prior to the Pliocene; Travoullion *et al.*, 2009), clarifying if and how arboreal taxa track their local environment is critical to improving our understanding of ancient environments in Australia. The common brushtail possum (*Trichosurus vulpecula* Kerr, 1972) is widely distributed throughout Australia, present in all states and territories and throughout much of Australia's interior

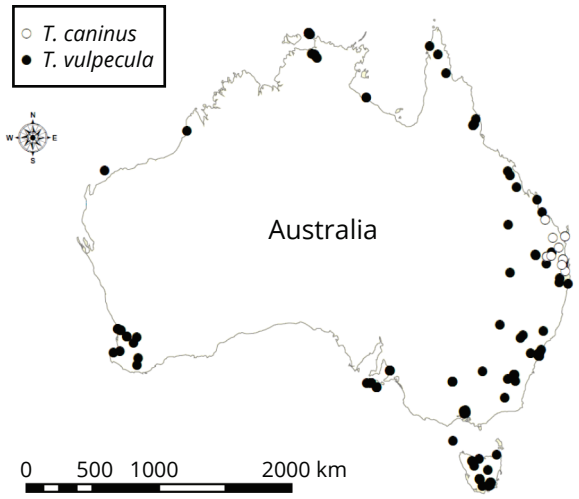

Figure 1.1: *Trichosurus vulpecula* was sampled from across Australia, while *Trichosurus caninus* was sampled throughout its range in the state of Queensland.

(Cruz, Sutherland, Martin, & Leung, 2012; Figure 1.1). Other brushtail possum species are less widespread, *e.g.* the short–eared brushtail possum, *Trichosurus caninus* Ogilby, 1836, which is found only in eastern Queensland and north-east New South Wales (Lindenmayer, Dubach, & Viggers, 2002; Figure 1.1). Here, we characterize the stable isotope and dental microwear signatures of both *T. vulpecula* and *T. caninus* and examine relationships between these proxy measurements and direct and/or proxy measurements of climate and environment.

We hypothesize that *Trichosurus* Lesson (1828) δ^{18}O values are negatively correlated with relative humidity and/or mean annual precipitation and δ^{13}C values are negatively correlated with enhanced vegetation index (EVI; a measure of canopy reflectance, or 'greenness' that is correlated with gross primary productivity (GPP; Glenn, Huete, Nagler, & Nelson, 2008; Sims *et al.*, 2006); GPP may correlate more habitable environments and more nutritious dietary items). Additionally, there is much debate regarding if dental microwear reflects diet or grit from food items (*e.g.* Ungar, Grine, & Teaford, 2008; DeSantis, 2016; Merceron *et al.*, 2016; Xia *et al.*, 2015); thus, we test if grit is responsible for microwear formation. Specifically, we test the hypothesis that brushtail possums will have higher com-

plexity values in more arid environments (*i.e.* lower relative humidity and/or lower mean annual precipitation), if grit is largely responsible for dental microwear formation. Lastly, we also test if increased body size (as inferred from jaw length measurements) is positively correlated with increased anisotropy and decreased complexity values (as larger subspecies of *T. vulpecula* are typically more folivorous than smaller subspecies (Cruz *et al.*, 2012)). By understanding how extant marsupials track diverse environments and climates, we can improve our understandings of the ecology and paleobiology of their fossil relatives. In turn, this can aid in reconstructing long-term responses of marsupials to changing climates, including the aridification and subsequent opening up of the Australian landscape since the mid–Cenozoic.

1.2 Methods

1.2.1 Specimens

Stable isotope samples and dental microwear molds were collected from extant specimens of *T. caninus* (n = 16) and *T. vulpecula* (n = 169) with associated locality and collection information. The geographic range of *T. caninus* is limited to the state of Queensland and northern New South Wales; however, the geographic range of *T. vulpecula* spans all Australian states and territories. Specimens were collected from across the range of each species with the exception of *T. caninus* from New South Wales (Figure 1.1). Specimens are housed at the American Museum of Natural History, New York City, NY, USA (AMNH), the Australian Museum, Sydney, NSW, AU (AM), the Australian National Wildlife Collection, Canberra, ACT, AU (ANWC), the Museum Victoria, Melbourne, VIC, AU (NMV), the Queensland Museum, Brisbane, QLD, AU (QM), the Tasmanian Museum and Art Gallery, Hobart, TAS, AU (TMAG), and the Western Australian Museum, Perth, WA, AU (WAM).

1.2.2 Dental microwear texture analysis

The wear facets of the left or right lower toothrow (p3 – m4) of each specimen were cleaned with 100% acetone and molded with a polyvinylsiloxane dental impression material (President's Jet, Coltene-Whaledent Corp., Alstatten, CHE). Dental casts were prepared at Vanderbilt University (Nashville, TN, USA) using Epotek 301 epoxy (Epoxy Technologies Corp., Billerica, MA, USA). After curing for at least 72 hours, the casts were scanned under 100x magnification on the Sensofar PLμ NEOX optical 3D surface profiler at Vanderbilt University, using previously established methods developed by Unga *et al.*, (2003), Scott *et al.*(2005), Scott *et al.*(2006), and slightly modified following Jones & DeSantis (2017) to maintain comparability between confocal microscopes (see Arman *et al.*, 2016). Four adjacent scans with a total area of 204 $\times$ 276 μm^2 were imaged and analyzed using scale-sensitive fractal analysis (ToothFrax and SFrax, Surfract Corp., www.surfract.com) to calculate the median values of the DMTA attribute variables anisotropy and complexity. Anisotropy, or exact proportion Length-scale anisotropy of relief (*epLsar*), is a measure of the directionality of features on a surface and is correlated with greater consumption of tough foods (*e.g.* leaves or grasses; Scott *et al.*, 2005, Scott *et al.*, 2006; DeSantis, 2016; Hedberg & DeSantis, 2017; DeSantis, Field, Rowe, & Dodson, 2017; Prideaux *et al.*2009). Complexity, or area-scale fractal complexity (*Asfc*), is a measure of changes in surface roughness at difference scales; higher values indicate consumption of harder or more brittle foods like fruits and/or seeds (Scott *et al.*, 2005, Scott *et al.*, 2006; DeSantis, 2016; Prideaux *et al.*, 2009).

1.2.3 Stable isotope analysis

A Dremel-style drill and carbide drill bits were used to sample enamel from the buccal surface of the left or right lower incisor. The dentition of *Trichosurus* specimens is small (with the m_1 of included specimens ranging in length from 0.44 to 0.64 cm), mak-

ing molar enamel collection highly destructive in contrast to incisors which are larger and contain less diagnostic morphological information. Although incisors may have formed while consuming the mother's milk and/or during weaning (*i.e.* reflecting, in part, the mother's dietary signal), the effect of the mother's milk is likely to be a consistent issue for all of the specimens sampled. As we are only comparing possums to one another, this should not be an issue and is consistent with prior work (DeSantis & Hedberg, 2017; Fraser, 2005). The enamel samples were subsequently prepared for analysis at Vanderbilt University where they were reacted with 30% hydrogen peroxide for at least 24 hours to remove organic material and 0.1 N acetic acid for 18 hours to remove secondary carbonates (similar to DeSantis & Hedberg, 2017). Approximately 1mg of each sample was analyzed on the VG Prism stable isotope ratio mass spectrometer in the Department of Geological Sciences at the University of Florida, internally calibrated against NBS-19, and reported in conventional delta notation where δ^{18}O, δ^{13}C = (R_{sample} / $R_{standard}$ 1) x 1000, where R = ^{18}O/^{16}O or ^{13}C/^{12}C ratio. Stable carbon is reported following the Vienna Convention (Coplen, 1994) in reference to the Pee Dee Belemnite (V-PDB) and stable oxygen values were converted to standard mean ocean water (V-SMOW) using the equation $\delta^{18}O_{V-SMOW}$ = 1.03086 * $\delta^{18}O_{VPDB}$ + 30.86 (Friedman & O'Neil, 1977).

1.2.4 Specimen, geographic, and environmental data

All specimens analyzed have locality data, either GPS coordinates (latitude and longitude data) or written descriptions of locations (*e.g.* 'Atherton Tableland, 6 mi. S.W. Ravenshoe, Queensland' which were converted to GPS coordinates using the WGS 84 datum). The elevation of all coordinate locations were identified using Google Earth Pro (© 2017 Google). Other information, such as collection date are available on a specimen-by-specimen basis and were collected from individual specimen labels and/or databases, including the Atlas of Living Australia (http://www.ala.org.au) and Vertnet (http://vertnet.org). The length of each mandible and m_1 examined were measured from digital photographs

containing scale bars using ImageJ (Rasband, W.S., ImageJ, U. S. National Institutes of Health, Bethesda, Maryland, USA, https://imagej.nih.gov/ij/, 1997-2018.).

Environmental variables, including modeled δ^{18}O values of local rainfall, climate information, and vegetation greenness were collected using publicly available resources. The Online Isotopes in Precipitation Calculator at waterisotopes.org was used to determine the stable oxygen isotope signature of precipitation ($\delta^{18}O_{meteoric}$) at each location (Bowen, 2018; Bowen & Revenaugh, 2003; Bowen, Wassenaar, & Hobson, 2005; IAEA/WMO, 2015). Mean annual precipitation (MAP, mm) and maximum and minimum mean annual temperature (max. MAT and min. MAT, respectively; °C) data were collected from the Australian Government Bureau of Meteorology weather station closest to each location that possessed at least a decade of records between 1955 and 1995 (Australian Government, 2018; http://www. bom.gov.au/climate/data/). When possible (and as was typically the case in 86% of all specimens for which temperature data were collected), thirty–year averages from 1961–1990 were used. Average relative humidity data from the period of 1983 to 2007 were obtained from the NASA Langley Research Center Atmospheric Science Data Center Surface meteorological and Solar Energy (SSE) web portal supported by the NASA LaRC POWER Project (https://asdc-arcgis.larc.nasa.gov/portal/home/item.html?id=1c1671fb53-c94dfdae57d4fd55c0e708). Enhanced Vegetation Index (EVI) or 'greenness' data was used as a proxy for primary productivity of a locality (Glenn *et al.*, 2008; Sims *et al.*, 2006) and was calculated over the period from January 2001 to December 2015 using the MODIS-/Terra Vegetation Indices Monthly L3 Global 0.05 Deg CMG V006 dataset (Didan, 2015).

1.2.5 Statistical analysis and model development

All analyses were performed in R version 3.2.1 (R core development team) initialized in R STUDIO version 1.1.442 using the following packages: 'dplyr' (Wickham, Francois, Henry, Mller, 2017), 'Hmisc' (Harrell, 2018), and 'psych' (Revelle, 2018). The packages 'raster' (Hijmans, 2017), 'rgdal' (Bivand, Keitt, & Rowlingson, 2018), and 'map-

		T. caninus	*T. vulpecula*	NSW	NT	QLD	SA	TAS	VIC	WA
	n	16	144	26	12	40	27	19	14	9
δ^{18}O	mean	30.9	30.9	31.6	30.6	31.7	29.8	29.5	31.8	31.4
	sd	1.3	2.2	1.8	2.1	2.4	1.7	1.7	1.6	1.6
	median	30.2	30.8	31.5	30.7	31.6	29.7	28.8	31.6	30.7
	min	29.4	26.5	28.1	26.5	27.0	27.2	27.2	29.1	29.5
	max	34.0	38.2	35.8	34.0	38.2	32.6	33.0	34.5	33.6
	range	4.7	11.7	7.7	7.5	11.2	5.4	5.8	5.4	4.1
	normality (*p*)	0.026	0.033	0.754	0.960	0.018	0.078	0.044	0.822	0.156
δ^{13}C	mean	-16.3	-15.9	-15.8	-15.3	-15.6	-16.9	-16.9	-14.8	-15.2
	sd	0.9	1.5	1.8	0.7	1.5	0.7	1.1	0.8	1.1
	median	-16.6	-16.1	-16.3	-15.3	-15.9	-16.8	-16.9	-14.5	-15.4
	min	-17.8	-19.2	-18.5	-16.4	-17.8	-18.4	-19.2	-16.0	-16.1
	max	-14.5	-9.1	-9.1	-14.3	-10.1	-15.2	-15.1	-13.5	-13.4
	range	3.3	10.1	9.4	2.1	7.8	3.2	4.1	2.5	2.7
	normality (*p*)	0.859	< 0.001	< 0.001	0.492	0.002	0.888	0.767	0.067	0.022
	n	16	144	23	11	40	33	14	25	14
Asfc	mean	2.32	2.89	2.92	2.51	2.52	3.11	3.62	3.15	1.81
	S,d	1.23	1.83	1.82	1.54	1.58	1.84	1.81	2.19	0.98
	median	2.08	2.57	2.74	1.91	2.25	2.74	3.00	2.11	1.45
	min	0.66	0.59	0.77	1.09	0.59	1.09	1.28	0.62	0.62
	max	5.63	9.47	9.47	6.03	7.35	8.61	7.54	8.67	3.88
	range	4.97	8.88	8.70	4.94	6.76	7.53	6.26	8.05	3.26
	normality (*p*)	0.655	< 0.001	0.038	0.031	0.336	0.003	0.009	0.003	0.425
epLsar	mean	0.0042	0.0035	0.0033	0.0038	0.0038	0.0033	0.0031	0.0036	0.0039
	sd	0.0017	0.0015	0.0017	0.0021	0.0018	0.0013	0.0014	0.0013	0.0012
	median	0.0042	0.0032	0.0029	0.0032	0.0040	0.0032	0.0024	0.0034	0.0038
	min	0.0009	0.0010	0.0011	0.0018	0.0009	0.0017	0.0017	0.0022	0.0024
	max	0.0077	0.0088	0.0076	0.0088	0.0081	0.0068	0.0056	0.0072	0.0060
	range	0.0068	0.0077	0.0065	0.0070	0.0072	0.0051	0.0039	0.0050	0.0036
	normality (*p*)	0.861	< 0.001	0.053	0.018	0.012	0.098	0.109	0.003	0.625

Table 1.1: Descriptive statistics for *T. vulpecula*, *T. caninus*, and all *Trichosurus* in each Australian state or territory.

tools' (Bivand & Lewin-Koh, 2017) were used for relative humidity and EVI data extraction from spatial files, while the packages 'ggplot2' (Wickham, 2009) and 'gridExtra' (Auguie, 2017) were used to visualize data. Descriptive statistics and Shapiro-Wilke tests of normality were calculated at the species and state levels for δ^{18}O, δ^{13}C, complexity (*Asfc*), and anisotropy (*epLsar*). Normally-distributed data were compared using a two-sample Student's T-test, while non-normally-distributed data were compared using

a Mann-Whitney U-test. When *T. caninus* specimens were compared to a subset of *T. vulpecula* specimens from the same region (latitudes between 24 and 28 °S, and longitudes between 150 and 153 °E), *T. caninus* has significantly lower δ^{18}O values than *T. vulpecula* ($\delta^{18}O_{T.vulpecula,subregion}$ $\bar{x}$ = 33.6 ‰, t = 2.7059, p = 0.022; Table **??**). Due to this difference, oxygen isotopes were modeled at both the species and genus level. All other variables (*i.e.* carbon isotopes and DMTA attribute values) were not significantly different between the two species and were modeled only at the genus level. Correlation coefficients between stable isotope and DMTA variables and specimen collection year, toothrow length, and m_1 length were calculated. Single and mixed variable linear regression models between carbon and oxygen isotope or microwear attribute values (*Asfc* and *epLsar*) and environmental variables (MAP, max. MAT, min. MAT, RH, EVI) were developed in R. Only max. MAT is used in constructing multiple linear regressions models, as it was more tightly correlated with isotopic and microwear values compared to min. MAT. Aikike's information criteria (AIC) is used to determine the best performing models; R^2, and *p* values are reported. All models and associated statistics are noted in Tables 1-3 and Supplementary Table S4-S6.

1.3 Results

All results are noted in Figs. 1.2–1.4, Tables 1.1–1.3, and Supplemental Tables 1.4–1.6. An α of 0.05 is applied when determining the significance of all *p*–values.

1.3.1 Modeling stable isotopes

When all *Trichosurus* taxa are combined, δ^{18}O values are best modeled by a combination of max. MAT, MAP, and MARH (Table 1.2). EVI, MAP, and MARH are positively correlated with δ^{18}O enamel values, while max. MAT is negatively correlated with δ^{18}O values (Table 1.2). When analyzing the two species separately, *T. vulpecula* δ^{18}O is best predicted by a model of max. MAT and MARH, while AIC values indicate *T. caninus* δ^{18}O is best predicted by max MAT, MAP, MARH, EVI and $\delta^{18}O_{meteoric}$ (Table 1.5). Stable car-

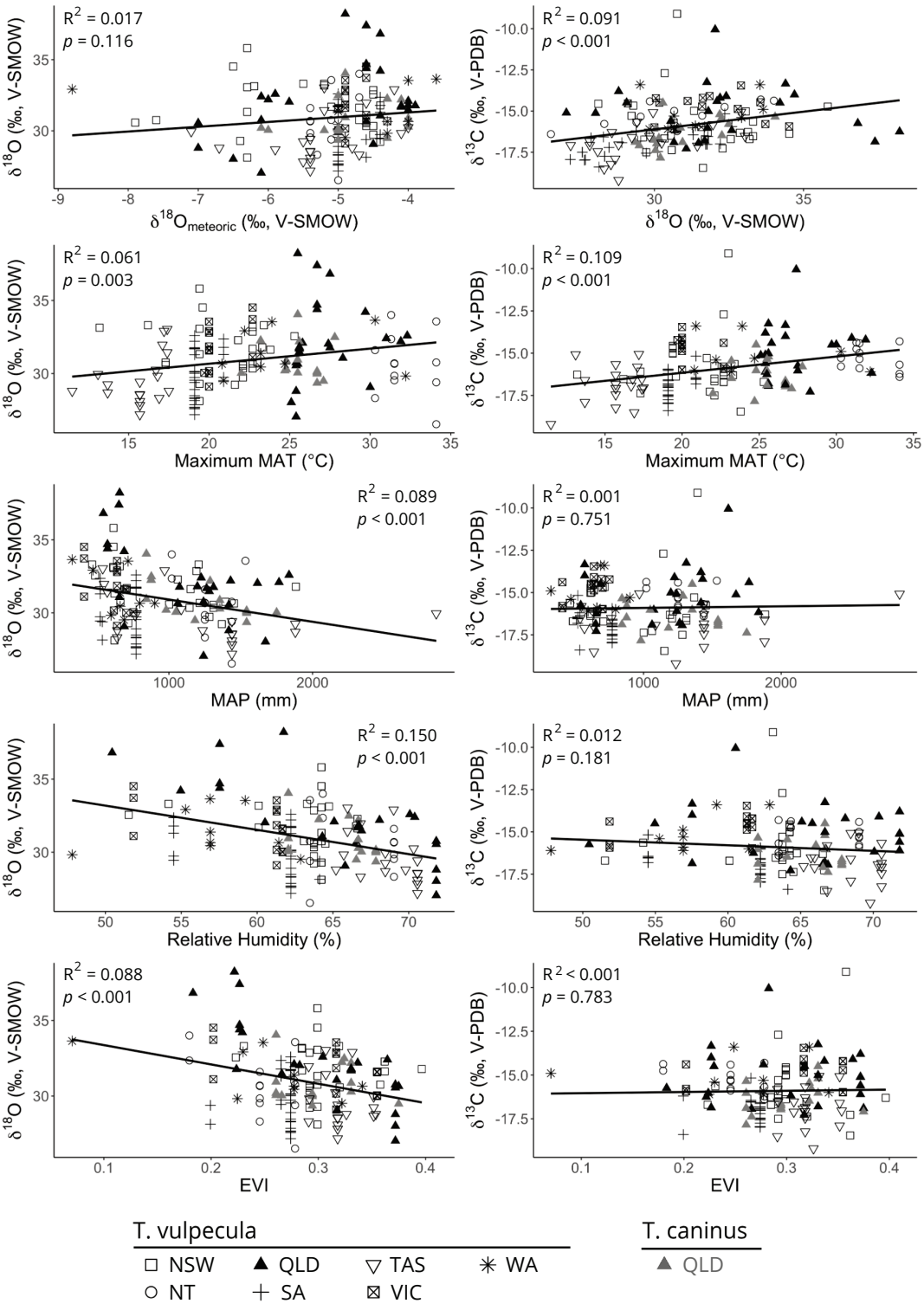

Figure 1.2: Stable oxygen and stable carbon compared to environmental variables.

	$\delta^{18}O$				$\delta^{13}C$			
	AIC	Δ	R^2	*p*	AIC	Δ	R^2	*p*
Latitude	636.84	28.55	0.018	0.104	518.29	9.81	0.078	< 0.001*
MAT	630.32	22.04	0.061	0.003*	513.21	4.73	0.109	< 0.001*
MAP	625.81	17.52	0.089	< 0.001*	530.14	21.66	0.001	0.751
MARH	615.63	7.35	0.150	< 0.001*	528.43	19.95	0.012	0.181
EVI	626.00	17.72	0.088	< 0.001*	530.17	21.69	0.001	0.783
$\delta^{18}O_{meteoric}$	637.02	28.74	0.017	0.116	530.23	21.74	<0.001	0.892
MAT + MAP	612.97	4.69	0.177	< 0.001*	515.11	6.63	0.110	< 0.001*
MAT + MARH	608.83	0.55	0.199	< 0.001*	513.87	5.39	0.117	< 0.001*
MAT + EVI	623.31	15.03	0.117	< 0.001*	512.74	4.26	0.124	< 0.001*
MAT + $\delta^{18}O_{meteoric}$	631.06	22.78	0.069	0.006*	514.44	5.96	0.114	< 0.001*
MAP + MARH	617.11	8.83	0.153	< 0.001*	527.73	19.25	0.030	0.110
MAP + EVI	621.93	13.65	0.125	< 0.001*	532.12	23.64	0.001	0.939
MAP + $\delta^{18}O_{meteoric}$	626.59	18.31	0.097	< 0.001*	532.13	23.65	0.001	0.947
MARH + EVI	615.96	7.67	0.160	< 0.001*	528.89	20.41	0.023	0.193
MARH + $\delta^{18}O_{meteoric}$	617.51	9.23	0.151	< 0.001*	530.15	21.67	0.014	0.359
EVI + $\delta^{18}O_{meteoric}$	627.38	19.10	0.092	< 0.001*	532.16	23.68	0.001	0.960
MAT + MAP + MARH	608.28	0.00	0.213	< 0.001*	515.44	6.96	0.120	< 0.001*
MAT + MAP + EVI	613.81	5.53	0.183	< 0.001*	513.18	4.70	0.133	< 0.001*
MAT + MAP + $\delta^{18}O_{meteoric}$	614.82	6.54	0.177	< 0.001*	516.20	7.72	0.115	< 0.001*
MAT + MARH + EVI	610.63	2.35	0.201	< 0.001*	508.48	0.00	0.161	< 0.001*
MAT + MARH + $\delta^{18}O_{meteoric}$	610.82	2.54	0.199	< 0.001*	514.34	5.86	0.127	< 0.001*
MAT + EVI + $\delta^{18}O_{meteoric}$	625.00	16.72	0.118	< 0.001*	514.40	5.92	0.126	< 0.001*
MAP + MARH + EVI	617.56	9.28	0.162	< 0.001*	528.47	19.99	0.039	0.131
MAP + MARH + $\delta^{18}O_{meteoric}$	618.97	10.68	0.154	< 0.001*	529.37	20.89	0.033	0.190
MAP + EVI + $\delta^{18}O_{meteoric}$	623.49	15.21	0.127	< 0.001*	534.11	25.63	0.001	0.988
MARH + EVI + $\delta^{18}O_{meteoric}$	617.91	9.63	0.160	< 0.001*	530.73	22.25	0.024	0.330
MAT + MAP + MARH + EVI	610.25	1.97	0.213	< 0.001*	510.44	1.96	0.161	< 0.001*
MAT + MAP + MARH + $\delta^{18}O_{meteoric}$	610.27	1.98	0.213	< 0.001*	515.90	7.42	0.129	< 0.001*
MAT + MAP + EVI + $\delta^{18}O_{meteoric}$	615.75	7.47	0.183	< 0.001*	514.67	6.19	0.136	< 0.001*
MAT + MARH + EVI + $\delta^{18}O_{meteoric}$	612.61	4.33	0.201	< 0.001*	509.27	0.79	0.168	< 0.001*
MAP + MARH + EVI + $\delta^{18}O_{meteoric}$	619.51	11.22	0.162	< 0.001*	530.24	21.76	0.040	0.211
MAT + MAP + MARH + EVI + $\delta^{18}O_{meteoric}$	612.23	3.95	0.213	< 0.001*	511.23	2.75	0.168	< 0.001*

Table 1.2: Models predicting stable isotope values for all *Trichosurus*. Here, MAT refers to max. MAT. Asterisks indicate significance at $\alpha = 0.05$, while grey highlighted rows are the models with the lowest AIC score.

bon isotopes for all *Trichosurus* are best predicted by a combined model of max. MAT, MARH, and EVI, while the only single variable models to predict $\delta^{13}C$ are latitude and max. MAT (in order of increasing predictive power; Table 1.2). We also examined the relationship between stable isotope values and monthly environmental parameters (Table 1.4),

which vary in significance and predictability between months and variables. While there was no significiant correlation between possum size and stable oxygen values from tooth enamel (p = 0.117), toothrow length (p_3 –m_4) is negatively correlated with stable carbon isotope values (p = 0.005, R^2 = 0.081) and latitude (p <0.001, R^2 = 0.287). It should also be noted that latitude and max. MAT are also strongly correlated in this dataset (p <0.001, R^2 = 0.85).

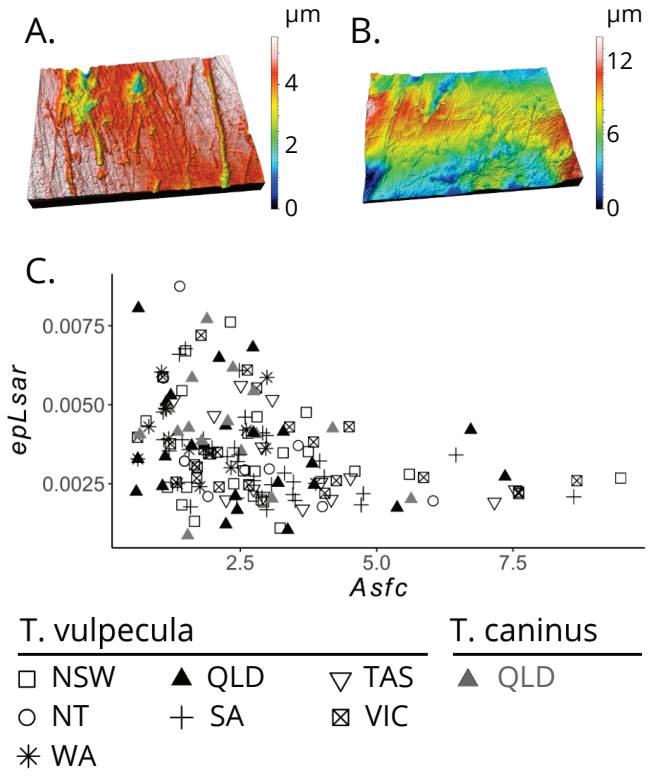

Figure 1.3: A. A high anisotropy dental microwear texture. *T. vulpecula*, right m_1, AMNH M160348. B. A high complexity dental microwear texture. *T. vulpecula*, left m_2, NMV C18837. C. Complexity (*Asfc*) compared to anisotropy (*epLsar*) of all *Trichosurus* specimens, including the two specimens shown in fig. 3a-b.

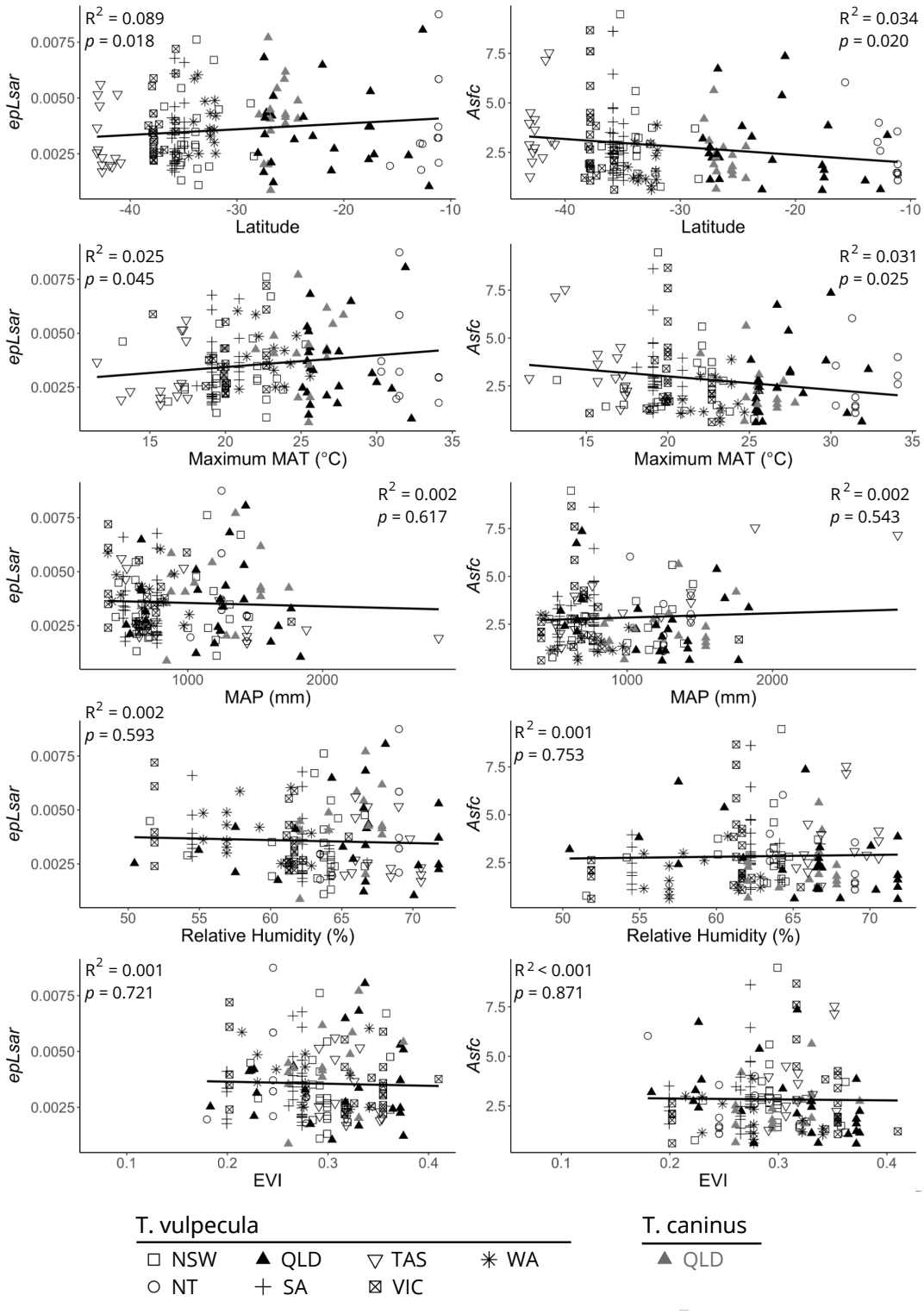

Figure 1.4: Anisotropy (*epLsar*) and complexity (*Asfc*) compared to environmental variables.

	Asfc				*epLsar*			
	AIC	Δ	R^2	*p*	AIC	Δ	R^2	*p*
Latitude	638.97	0.00	0.034	0.020*	-1614.51	1.13	0.018	0.089
MAT	639.39	0.42	0.031	0.025*	-1615.64	0.00	0.025	0.045*
MAP	644.13	5.16	0.002	0.543	-1611.82	3.82	0.002	0.617
MARH	644.41	5.44	0.001	0.753	-1611.85	3.79	0.002	0.593
EVI	644.48	5.51	< 0.001	0.871	-1611.69	3.95	0.001	0.721
MAT + MAP	639.52	0.56	0.043	0.033*	-1615.01	0.63	0.033	0.069
MAT + MARH	641.10	2.14	0.033	0.071	-1614.18	1.46	0.028	0.104
MAT + EVI	641.05	2.09	0.034	0.069	-1613.64	2.00	0.025	0.136
MAP + MARH	646.12	7.15	0.002	0.828	-1609.89	5.75	0.002	0.849
MAP + EVI	645.96	6.99	0.003	0.764	-1609.85	5.79	0.002	0.867
MARH + EVI	646.27	7.31	0.001	0.891	-1609.86	5.78	0.002	0.862
MAT + MAP + MARH	641.32	2.35	0.044	0.071	-1613.01	2.63	0.033	0.150
MAT + MAP + EVI	639.75	0.78	0.053	0.036*	-1613.34	2.30	0.035	0.130
MAT + MARH + EVI	642.09	3.13	0.039	0.099	-1612.37	3.27	0.030	0.195
MAP + MARH + EVI	647.96	8.99	0.003	0.910	-1607.9	7.74	0.002	0.953
MAT + MAP + MARH + EVI	641.75	2.78	0.053	0.074	-1611.37	4.27	0.036	0.226

Table 1.3: Models predicting DMTA values for all *Trichosurus*. Here, MAT refers to max. MAT. Asterisks indicate significance at $\alpha = 0.05$, while grey highlighted rows are the models with the lowest AIC score.

1.3.2 Modeling dental microwear textures

There are no differences in anisotropy and complexity between *Trichosurus caninus* and *Trichosurus vulpecula* specimens from the same latitudinal and longitudinal ranges, therefore all taxa were grouped together for model analysis. All possums have complexity (*Asfc*) values between 0.59 and 9.47 and anisotropy (*epLsar*) values between 0.0009 and 0.0088 (Table 1.1 and Figure 1.3). Complexity and anisotropy are best modeled by max. MAT (note that latitude has a stronger negative relationship with complexity than max. MAT; Table 1.3). When DMTA attribute values were matched to climate data from the month of specimen collection, mean maximum temperature is best predicted by complexity. No variables significantly modeled anisotropy (Table 1.6). There are also no significant correlations between possum size and anisotropy and complexity values ($p = 0.906$ and $p = 0.794$, respectively).

1.4 Discussion

1.4.1 Tracking climate and environment via stable isotopes

Stable oxygen values of *Trichosurus* enamel are comparable to those of other marsupials, including macropods, wombats, and koalas (Prideaux *et al.*, 2007, DeSantis & Hedberg, 2017); however, the range of *Trichosurus* δ^{18}O values reported here (Table **??**) is greater than that of koalas (which range between 31.2-34.4‰; DeSantis & Hedberg, 2017). *Trichosurus* are recording almost as wide of a range of oxygen isotopes as macropodids and vombatids (which is reported to be 23.4-39.7‰ byPrideaux *et al.*(2007)), but show no correlation with latitude (Table 1.1) unlike other marsupials. Max. MAT, which strongly co-varies with latitude in these specimens, is significantly related to *Trichosurus* δ^{18}O but only weakly so. *Trichosurus* δ^{18}O values from tooth enamel are significantly correlated with relative humidity, where MARH explains almost twice as much variation as MAP, yet both are negatively correlated with δ^{18}O enamel values (Figure 1.2, Table 1.2).

However, these negative relationships are consistently weaker than in other marsupials (Prideaux *et al.*, 2007; Murphy, 2007a; DeSantis & Hedberg, 2017). Prideaux *et al.*(2007) found that kangaroo δ^{18}O was higher in low rainfall climates than in moderate or high rainfall climates. Murphy *et al.* (2007a) demonstrated temperature is only effective at predicting kangaroo δ^{18}O when relative humidity is included in the model, and that this interaction explained over half the variation in δ^{18}O values. In koalas (*Phascolarctos cinereus*) from sites in Queensland and New South Wales, stable oxygen isotopes are best predicted by MAP and the δ^{18}O values of local meteoric water (DeSantis & Hedberg, 2017). This is expected for taxa who do not consume free-standing water (evaporation sensitive taxa using terms from (Levin *et al.*, 2006)), whose oxygen isotope signal is influenced by leaf evapotranspiration and thus reliant on relative humidity (Murphy *et al.*, 2007a; Farquhar & Lloyd; 1993). Both MAP and relative humidity were negatively correlated with possum δ^{18}O enamel values. However, *Trichosurus* stable oxygen isotopes are best predicted

by integrating all climatic variables (not EVI or $\delta^{18}O_{meteoric}$), demonstrating increased $\delta^{18}O$ enamel values with increased mean annual maximum temperatures and decreased mean annual precipitation and mean annual relative humidity (i.e. hotter and drier conditions). While this relationship only accounts for a fifth of the total variation present in this system, it does indicate that enamel stable oxygen isotopes in *Trichosurus* are capable of tracking relative aridity across the landscape. Thus, our first hypothesis is correct, despite the relationship between $\delta^{18}O$ and aridity being less strong than would be expected based on results in macropodids and phascolarctids. All arboreal marsupials so far examined show significant positive relationships with increasingly arid environments (i.e. lower MAP and/or relative humidity).

Small amounts of variation within *Trichosurus* stable oxygen values could be due to dietary variability between individuals. In other arboreal taxa, *e.g.* primates, consumption of leaves (versus fruits) and/or understory (versus canopy or sub-canopy) plant material can results in lower $\delta^{18}O$ values (Cerling *et al.*, 2004; Roberts, Blumenthal, Dittus, Wedage, & Lee-Thorp, 2017). Foraging height data for brushtail possums is sparse; *T. vulpecula* in QLD are reported to forage at canopy heights of 7–10m, while *T. caninus* is noted to include more understory plants in its diet (How, 1978; Laurance, Laurance, & Hilbert, 2008). This may contribute to the difference in average $\delta^{18}O$ value between *T. caninus* and *Trichosurus* sampled from the same subregion. However, variation within *Trichosurus* $\delta^{18}O$ values may also be due to the differences in the proportion of fruits and leaves in individuals diets. Roberts *et al.* (2017) reported that within the same forest consuming 100% fruits versus 100% leaves can result in 2‰ enrichment in $\delta^{18}O$. Additionally, flowers have a $\delta^{18}O$ signature intermediate to fruits and leaves (Roberts *et al.*, 2017). In the Northern Territory and Western Australia *Trichosurus* populations, flowers may contribute between 10 to 98% of a possums diet, with the rest being fruits and invertebrates, not leaves (Cruz *et al.*, 2012; Kerle, 1998; Molloy & Davis, 2017). However, in Queensland, *Trichosurus* consumes primarily leaves, with some individuals consuming between 30-45% of their diet in fruits

and flowers (Cruz *et al.*, 2012; DeGabriel, Moore, Foley, Johnson, 2009). In south eastern Australia, possums primarily consume foliage (Cruz *et al.*, 2012). These widespread differences in diet across the range of *Trichosurus* may contribute relatively small (<2‰) variation in brushtail possum stable oxygen values. Despite the minor influence of diet, it is apparent that possums appear to be 'evaporation sensitive' taxa (per Levin *et al.*, 2006), as they do track relative water deficits as inferred from MAP and relative humidity and are not significantly correlated with modeled $\delta^{18}O_{meteoric}$ values.

Brushtail possum stable carbon isotopes are poorly predicted by the environmental parameters tested here. Of the single variable models that significantly predicted $\delta^{13}C$, max. MAT was the strongest, followed by latitude (Table 1.2). Latitude and max. MAT positively co-vary as a regions temperature is strongly correlated with latitude ($p << 0.001$, $R = 0.85$). The multi-attribute model that best predicts $\delta^{13}C$ incorporates max MAT, MARH, and EVI (Table 1.2), which could cause (in the case of MAT and MARH) and reflect (in the case of EVI) differences in the floral communities between sites. Ecological niche modeling of *T. vulpecula* from southwest Australia shows a combined precipitation and temperature variable (specifically precipitation of the coldest month) strongly contributes towards model fit, but that annual precipitation has a greater effect (Molloy, Davis, & van Etten, 2016). Temperature and rainfall seasonality (mean temperature of the wettest quarter) has been identified as a key difference in the ecology of *T. caninus* and the more southern *Trichosurus cunninghami* (Fischer, Lindenmayer, Nix, Stein, & Stein, 2001). Interactions between precipitation and temperature appear to interactively affect brushtail possum ecology.

Other factors may also be contributing to the wide range of $\delta^{13}C$ values seen here (which range from -19.2 to -9.1‰). The lack of correlation between $\delta^{13}C$ and EVI suggests that possums are not tracking changes in local landscape greenness as per our second hypothesis. This instead indicates that even in more arid regions, *Trichosurus* is preferentially consuming C_3 vegetation from denser trees/shrubs than may be 'typical' of that environment. This is consistent with reports that brushtail possums in arid, naturally un–forested

central and semi–arid northern Australian areas will congregate around tree–lined creeks and canals (Burbridge, Johnson, Fuller, & Southgrate, 1988; Munks, Corkrey, & Foley, 1996). Possum δ^{13}C may reflect diet or the height at which vegetation is consumed in the forest canopy. Neither MARH, MAP, max. MAT, or a combination of these variables predict koala stable carbon isotopes; thus, koala δ^{13}C was interpreted as tracking canopy density and/or feeding height (DeSantis & Hedberg, 2017).

The range of δ^{13}C values presented here (Table 1.1) is within the range expected for diets composed of predominantly C_3 vegetation, but *Trichosurus* δ^{13}C values may be more difficult to interpret as brushtail possums have a greater dietary range than koalas, incorporating foliage as well as fruits, flowers, seeds, fungi, and animal material (e.g. Cruz *et al.*, 2012; DeGabriel *et al.*, 2009; Fulton, 2017; Gloury & Handasyde, 2015; How, 1978; How & Hillcox, 2000, Johnson, McQuillian, Kirkpatrick, 2011; Kerle, 1998). δ^{13}C enamel values are reflective of latitudinal temperature gradients and similarly track vegetation much like has been documented in horses and rodents (Cerling *et al.*, 1997; Morgan, Kingston, & Marino, 1994; MacFadden, Cerling, Harris, & Prado, 1999; Smiley, Cotton, Badgely, & Cerling, 2016). Non-foliage items such as fruit often have higher δ^{13}C values (approximately 1.1‰ or greater) than foliage from the same plants (Cernusak *et al.*, 2009; Roberts *et al.*, 2017), so possum diets with higher proportions of non-foliage items are expected to have more positive δ^{13}C values than possums eating a high foliage diet. Tasmanian and South Australian brushtail possums have lower δ^{13}C mean values than possums in other states and territories. Brushtail possums in these states are more folivorous than possums found elsewhere (Cruz *et al.*, 2012); a primarily folivorous diet may explain this variation. Additionally, possum body size (indicated by toothrow length) is significantly and negatively related to both δ^{13}C and latitude. *Trichosurus* has been found to follow Bergmann's Rule, which theorizes that endotherm body size decreases as latitude (and temperature) does (Bergmann, 1847; Kerle, McKay, & Sharman, 1991; Yom-Tov, Green, & Coleman, 2009). Decreases in possum body size associated with latitude and underlying temperature

gradients may make a more frugivorous and/or omnivorous diet more feasible in terms of locating higher quality food items and consuming enough to provide for the individuals energy requirements (Cruz *et al.*, 2012; Kerle *et al.*, 1991) which are higher per unit biomass than larger animals (Demment & Van Soest, 1985).

1.4.2 Dental microwear textures, climate, and diet

There is still much debate about whether microwear in herbivores is formed through interactions between dental enamel and exogenous grit, which is expected to vary with environmental conditions, or endogenous phytoliths, the amount of which consumed would vary with different diets (Ungar *et al.*, 2008 2008; DeSantis, 2016; Merceron *et al.*, 2016; Xia *et al.*, 2015). An analysis of *Paranthropous boisei*, a fossil hominin dubbed the Nutcracker Man for its large, apparently crushing dentition, reignited this debate when microwear across the species was found to indicate a tough, rather than hard (as expected) diet (Ungar *et al.*, 2008). However, experimental studies have shown that materials softer than enamel (e.g. aluminum, brass, and amorphous silica) can create wear patterns through enamel removal (Xia *et al.*, 2015), while experimental feeding studies showed grazing and browsing microwear signatures are preserved, even when diets have been supplemented with exogenous grit in sheep (Merceron *et al.*, 2016). In rabbits, seed consumption is not needed to form pitted textures, but can occur through phytolith contact with teeth instead; additionally, low-silica diets have more textural variation than high-silica diets (Schulz *et al.*, 2013). When examining wild-caught rodents in environments with different grit loads, Burgman, Leichliter, Avenant, & Ungar (2016) found a lack of consistent environmental effect on microwear variables, suggesting that differences in African rodent microwear textures were due to dietary flexibility and differences in available vegetation across the habitats examined. Microwear textures consistently correlate with diet across a range of mammalian taxa (e.g. ungulates, primates, rodents, and marsupials; DeSantis, 2016; Merceron *et al.*, 2016; Scott *et al.*, 2012; Xia *et al.*, 2015), even across large spatial scales.

However, the debate regarding dental microwear formation continues.

It was hypothesized that if abrasion via grit consumption is a primary mechanism of microwear formation, anisotropy would be positively related to increasingly arid conditions. However, there was no relationship between anisotropy and RH or MAP and only a very weak positive relationship with maximum MAT (Table 1.3, Figure 1.4), indicating that the possums microwear signal was not affected by warmer or drier conditions as per our third hypothesis. The relationship between anisotropy and temperature understandably mirrors the relationship between anisotropy and latitude in direction and magnitude; as discussed above, temperature and latitude co-vary strongly. This covariance is also seen in the relationship between complexity and temperature and latitude, though increasing complexity is negatively related to these attributes. Interestingly, there is no relationship between EVI and complexity or anisotropy, with possums consuming foods with similarly wide variation in toughness or hardness regardless of the type of environment they are occupying. This lack of correlation between climate/environment and microwear suggests that possum microwear is tracking the diets of the possums. Brushtail possum microwear is highly variable (Figure 1.3), with some individuals eating tough foods and others eating hard foods (as inferred from high epLsar or high Asfc values, respectively).

This variation in dietary strategies is expected, given the variety of food items (*e.g.* leaves, fruits, flowers, invertebrates, etc.; Cruz *et al.*, 2012; DeGabrie *et al.*, 2009, Fulton, 2017; Gloury & Handasyde, 2015; How, 1978; How & Hillcox, 2000, Johnson *et al.*, 2011; Kerle, 1998; Kerle, 2001) that are consumed by brushtail possums. Foliage is a major component of most *Trichosurus* individuals diets (DeGabriel *et al.*, 2009; Gloury & Handasyde, 2015; Kerle, 2001), yet few possums show high epLsar values of greater than 0.006 (8.6%) and low complexity signal (*Asfc* <2) that would indicate a predominantly folivorous diet (based on Hedberg & DeSantis, 2017 and Scott *et al.*, 2006). In comparison to koalas eating a primarily folivorous diet (Martin & Handasyde, 1999), possums have microwear signatures that are on average more complex and less anisotropic than koalas

(see Hedberg & DeSantis, 2017). However, at least some of the possums analyzed here have diets that are as anisotropic, and thus as tough as the toughest koala diets (Hedberg & DeSantis, 2017).

While possums are traditionally classified as folivores, *Trichosurus* microwear values are similar to those of *Cercocebus atys*, the frugivorous sooty mangabey (Scott, Teaford, & Ungar, 2012), and *Trichosurus* diets vary in the amount of foliage consumed across their range (Cruz *et al.*, 2012). At least 35% of *T. vulpecula*'s diet in southern Western Australian diet is foliage, followed by at least 20% flowers, and approximately 10% each of fruits and seeds (Cruz *et al.*, 2012). In Australias arid central region, acacia flowers and leaves, *Amyema maidenii* (mistletoe) leaves, and *Solanum centrale* fruits composed the majority of *T. vulpecula* diets, with $<1\%$ being eucalyptus foliage (Evans, 1992). *T. vulpecula* in northern Australia have also been reported to consume a diet high in mangrove fruits and flowers (Kerle, 1984; Kerle, 1985; Kerle & Burgman, 1984). In Queensland, *T. vulpecula* consumes higher degrees of foliage, with Cape York possum scat containing 80% leaf matter, while populations on Queenslands central coast spent 55-70% of their feeding time on foliage and the remainder on flowers and fruits (Freeland & Winter, 1975; Kerle, 1984; Proctor-Grey, 1984). Victorian population of *T. vulpecula* consumed up to 90% of its diet in eucalyptus leaves (Kerle, 1984). Similarly, populations across eastern Australia consumed large amounts of eucalyptus leaves (Owen & Thompson, 1965). The diets of Tasmanian *T. vulpecula* are predominantly folivorous, supplemented with fungi and minor amounts of flowers, fruits, and pollen (Fitzgerald, 1984; Statham, 1984). *T. caninus* consumes *Acacia* foliage and some understory plants (How, 1978). As possums are known to consume both hard and tough foods (e.g. fruits and leaves, respectively), the predominantly hard-food DMTA signature presented here suggests that hard-food consumption may overwrite the microwear textures produced when consuming tough-food items in possums. (It has also been suggested that abrasive foods may overwrite the microwear left by less abrasive foods, however this may apply more to ground-dwelling organism such as rodents and ungulates

(Schulz *et al.*, 2013).) This may be more expected in smaller possums, as there is evidence that smaller subspecies of *Trichosurus* have more varied diets (Cruz *et al.*, 2012). However, per our fourth hypothesis, neither anisotropy or complexity is significantly correlated to toothrow or m1 length. Experimental work with primates may help to resolve the details of dental microwear formation, although much can be learned from examining dental microwear relationships with climatic variables.

1.5 Conclusion

The brushtail possums analyzed here appear to track climatic conditions via stable isotopes in tooth enamel, including relative aridity via oxygen isotopes and temperature via carbon isotopes. In assemblages dominated by possums and/or other arboreal taxa, general climate conditions and local vegetative resources may be inferred. Conversely, the lack of relationships between dental microwear textures and climatic variables suggests that higher grit loads (as inferred to occur in drier and dustier environments) are not primary driver of dental microwear. Instead, brushtail possums have highly variable DMTA attribute values that suggest the consumption of tough and/or hard food items, consistent with observed diets including both foliage and fruits, flowers, and seeds. Proxies like stable isotope analysis and DTMA can provide an added layer of insight into the lives of organisms that could not otherwise be gained. Examining the paleoecology of fossil organisms and thier responses to climate and habitat alteration can help us understand not only the evolutionary trajectories of these organisms through deep time, but the driving forces behind these patterns.

SUPPLEMENTAL TABLES

	$\delta^{18}O$		$\delta^{13}C$		*Asfc*		*epLsar*	
	p	R	*p*	R	*p*	R	*p*	R
$\delta^{18}O_{meteoric}$ Jan	0.376	0.005	0.967	< 0.001*	-	-	-	-
$\delta^{18}O_{meteoric}$ Feb	< 0.001*	0.112	0.007*	0.049	-	-	-	-
$\delta^{18}O_{meteoric}$ Mar	0.037*	0.030	0.997	< 0.001*	-	-	-	-
$\delta^{18}O_{meteoric}$ Apr	0.007*	0.049	0.154	0.014	-	-	-	-
$\delta^{18}O_{meteoric}$ May	0.836	< 0.001*	0.073	0.022	-	-	-	-
$\delta^{18}O_{meteoric}$ Jun	0.810	< 0.001*	0.078	0.021	-	-	-	-
$\delta^{18}O_{meteoric}$ Jul	0.523	0.003	0.250	0.009	-	-	-	-
$\delta^{18}O_{meteoric}$ Aug	0.387	0.005	0.357	0.006	-	-	-	-
$\delta^{18}O_{meteoric}$ Sept	0.766	< 0.001*	0.045*	0.027	-	-	-	-
$\delta^{18}O_{meteoric}$ Oct	0.017*	0.038	< 0.001*	0.091	-	-	-	-
$\delta^{18}O_{meteoric}$ Nov	0.820	< 0.001*	0.799	< 0.001*	-	-	-	-
$\delta^{18}O_{meteoric}$ Dec	0.307	0.007	0.124	0.016	-	-	-	-
$\delta^{18}O_{meteoric}$ Annual	0.116	0.017	0.892	< 0.001*	-	-	-	-
MT max Jan	< 0.001*	0.160	< 0.001*	0.127	0.004*	0.053	0.061	0.022
MT max Feb	< 0.001*	0.151	< 0.001*	0.129	0.007*	0.045	0.068	0.021
MT max Mar	< 0.001*	0.123	< 0.001*	0.136	0.012*	0.040	0.039*	0.027
MT max Apr	0.003*	0.059	< 0.001*	0.101	0.045*	0.025	0.054	0.023
MT max May	0.038*	0.029	< 0.001*	0.092	0.053*	0.024	0.049*	0.024
MT max Jun	0.123	0.016	< 0.001*	0.081	0.057	0.023	0.057	0.023
MT max Jul	0.144	0.015	< 0.001*	0.080	0.061	0.022	0.055	0.023
MT max Aug	0.088	0.020	< 0.001*	0.089	0.067	0.021	0.057	0.023
MT max Sept	0.016*	0.039	< 0.001*	0.099	0.067	0.021	0.056	0.023
MT max Oct	0.003*	0.059	< 0.001*	0.107	0.047	0.025	0.060	0.022
MT max Nov	< 0.001*	0.084	< 0.001*	0.114	0.016*	0.036	0.051	0.024
MT max Dec	< 0.001*	0.129	< 0.001*	0.129	0.006*	0.047	0.045*	0.025
MT max Annual	0.003*	0.061	< 0.001*	0.109	0.025*	0.031	0.045*	0.025
MT min Jan	0.001*	0.071	< 0.001*	0.128	0.086	0.019	0.029*	0.030
MT min Feb	0.002*	0.064	< 0.001*	0.125	0.090	0.018	0.026*	0.031
MT min Mar	0.016*	0.039	< 0.001*	0.113	0.115	0.016	0.031*	0.029
MT min Apr	0.250	0.009	< 0.001*	0.088	0.180	0.011	0.043*	0.026
MT min May	0.832	< 0.001*	0.001*	0.070	0.223	0.009	0.062	0.022
MT min Jun	0.741	< 0.001*	0.003*	0.059	0.270	0.008	0.080	0.019
MT min Jul	0.553	0.002	0.004*	0.054	0.292	0.007	0.100	0.017
MT min Aug	0.865	< 0.001*	0.001*	0.068	0.324	0.006	0.104	0.017

Table 1.4: Relationships between stable isotope and microwear variables and all individual annual and monthly variables. Asterisks indicate significance with an $\alpha = 0.05$. Dashes indicate the relationship was not tested.

	$\delta^{18}O$		$\delta^{13}C$		*Asfc*		*epLsar*	
	p	R	*p*	R	*p*	R	*p*	R
MT min Sept	0.500	0.003	< 0.001*	0.085	0.289	0.007	0.080	0.019
MT min Oct	0.093	0.019	< 0.001*	0.102	0.231	0.009	0.067	0.021
MT min Nov	0.025*	0.034	< 0.001*	0.112	0.157	0.013	0.051	0.024
MT min Dec	0.004*	0.055	< 0.001*	0.122	0.119	0.015	0.038*	0.027
MT min Annual	0.164	0.013	< 0.001*	0.098	0.177	0.012	0.047*	0.025
MP Jan	0.702	0.001	0.005*	0.054	0.227	0.009	0.264	0.008
MP Feb	0.745	< 0.001*	0.001*	0.069	0.243	0.009	0.341	0.006
MP Mar	0.264	0.009	0.003*	0.059	0.447	0.004	0.655	0.001
MP Apr	< 0.001*	0.075	0.919	< 0.001*	0.406	0.004	0.640	0.001
MP May	< 0.001*	0.134	0.020*	0.037	0.150	0.013	0.323	0.006
MP Jun	< 0.001*	0.123	0.002*	0.063	0.181	0.011	0.172	0.012
MP Jul	< 0.001*	0.120	< 0.001*	0.097	0.088	0.018	0.076	0.020
MP Aug	< 0.001*	0.125	< 0.001*	0.104	0.020*	0.034	0.026*	0.031
MP Sept	< 0.001*	0.127	< 0.001*	0.079	0.004*	0.052	0.009*	0.043
MP Oct	0.019*	0.038	0.059	0.024	0.018*	0.035	0.173	0.012
MP Nov	0.033*	0.031	0.791	< 0.001*	0.450	0.004	0.670	0.001
MP Dec	0.741	< 0.001*	0.036*	0.030	0.723	< 0.001*	0.602	0.002
MP Annual	< 0.001*	0.089	0.751	< 0.001*	0.543	0.002	0.617	0.002
EVI Jan	0.177	0.013	0.112	0.017	0.357	0.005	0.793	< 0.001*
EVI Feb	0.421	0.004	0.045	0.028	0.319	0.006	0.719	< 0.001*
EVI Mar	0.310	0.007	0.046*	0.027	0.387	0.005	0.717	< 0.001*
EVI Apr	0.038*	0.029	0.136	0.015	0.525	0.003	0.903	< 0.001*
EVI May	< 0.001*	0.105	0.742	< 0.001*	0.997	< 0.001*	0.689	0.001
EVI Jun	< 0.001*	0.175	0.354	0.006	0.695	< 0.001*	0.448	0.004
EVI Jul	< 0.001*	0.158	0.060	0.024	0.765	< 0.001*	0.547	0.002
EVI Aug	< 0.001*	0.082	0.052	0.026	0.843	< 0.001*	0.796	< 0.001*
EVI Sept	0.009*	0.046	0.142	0.015	0.721	< 0.001*	0.729	< 0.001*
EVI Oct	0.002*	0.067	0.279	0.008	0.436	0.004	0.398	0.005
EVI Nov	0.006*	0.052	0.725	< 0.001*	0.477	0.003	0.284	0.007
EVI Dec	0.100	0.019	0.325	0.007	0.829	< 0.001*	0.778	< 0.001*
EVI Annual	< 0.001*	0.088	0.783	< 0.001*	0.871	< 0.001*	0.721	< 0.001*
RH Jan	0.027*	0.033	0.771	< 0.001*	0.850	< 0.001*	0.731	< 0.001*
RH Feb	0.111	0.017	0.534	0.003	0.749	< 0.001*	0.768	< 0.001*
RH Mar	0.004*	0.055	0.914	< 0.001*	0.834	< 0.001*	0.857	< 0.001*
RH Apr	< 0.001*	0.101	0.317	0.007	0.788	< 0.001*	0.775	< 0.001*
RH May	0.077	0.021	0.170	0.013	0.414	0.004	0.171	0.012

Table 1.4: Cont'd. Relationships between stable isotope and microwear variables and all individual annual and monthly variables. Asterisks indicate significance with an $\alpha = 0.05$.

	$\delta^{18}O$		$\delta^{13}C$		*Asfc*		*epLsar*	
	p	R	*p*	R	*p*	R	*p*	R
RH Jun	0.510	0.003	0.160	0.014	0.420	0.004	0.141	0.014
RH Jul	0.282	0.008	0.048*	0.027	0.419	0.004	0.136	0.014
RH Aug	0.001*	0.068	0.008*	0.048	0.480	0.003	0.295	0.007
RH Sept	< 0.001*	0.232	0.008*	0.048	0.668	0.001	0.740	< 0.001*
RH Oct	< 0.001*	0.247	0.414	0.005	0.907	< 0.001*	0.991	< 0.001*
RH Nov	< 0.001*	0.111	0.985	< 0.001*	0.864	< 0.001*	0.735	< 0.001*
RH Dec	0.005*	0.053	0.181	0.012	0.753	< 0.001*	0.593	0.002
RH Annual	< 0.001*	0.150	0.160	0.014	0.420	0.004	0.141	0.014
MT max matched	-	-	-	-	0.120	0.021	0.367	0.007
MT min matched	-	-	-	-	0.121	0.021	0.706	0.001
MP matched	-	-	-	-	0.936	< 0.001*	0.537	0.003
EVI matched	-	-	-	-	0.416	0.006	0.937	< 0.001*
RH matched	-	-	-	-	0.451	0.004	0.164	0.012

Table 1.4: Cont'd. Relationships between stable isotope and microwear variables and all individual annual and monthly variables. Asterisks indicate significance with an $\alpha = 0.05$. Dashes indicate the relationship was not tested.

	T. vulpecula				*T. caninus*			
	AIC	Δ	R^2	*p*	AIC	Δ	R^2	*p*
Latitude	577.54	25.05	0.020	0.111	59.25	12.77	0.015	0.651
MAT	570.76	18.27	0.069	0.002*	59.01	12.53	0.030	0.523
MAP	568.98	16.48	0.015	0.161	50.61	4.13	0.028	0.534
MARH	558.55	6.05	0.082	< 0.001*	56.20	9.72	0.426	0.006*
EVI	566.76	14.26	0.152	< 0.001*	59.49	13.01	0.186	0.095
$\delta^{18}O_{meteoric}$	578.11	25.61	0.097	< 0.001*	58.24	11.76	< 0.001*	0.995
MAT + MAP	557.50	5.00	0.015	0.160	52.08	5.60	0.076	0.303
MAT + MARH	552.50	0.00	0.171	< 0.001*	58.17	11.69	0.445	0.022*
MAT + EVI	564.41	11.91	0.202	< 0.001*	60.99	14.51	0.188	0.259
MAT + $\delta^{18}O_{meteoric}$	571.81	19.32	0.127	< 0.001*	59.87	13.39	0.031	0.816
MAP + MARH	560.29	7.80	0.076	0.006*	51.68	5.20	0.097	0.517
MAP + EVI	564.67	12.17	0.154	< 0.001*	52.60	6.12	0.458	0.019*
MAP + $\delta^{18}O_{meteoric}$	570.25	17.75	0.125	< 0.001*	49.98	3.50	0.427	0.027*
MARH + EVI	558.51	6.01	0.087	0.003*	57.03	10.55	0.513	0.009*
MARH + $\delta^{18}O_{meteoric}$	560.55	8.05	0.165	< 0.001*	52.88	6.40	0.244	0.163
EVI + $\delta^{18}O_{meteoric}$	568.64	16.14	0.152	< 0.001*	58.16	11.68	0.416	0.030*
MAT + MAP + MARH	552.85	0.35	0.098	0.001*	51.82	5.34	0.188	0.258
MAT + MAP + EVI	558.19	5.69	0.212	< 0.001*	54.03	7.55	0.518	0.028*
MAT + MAP + $\delta^{18}O_{meteoric}$	559.46	6.97	0.180	< 0.001*	51.61	5.13	0.447	0.061
MAT + MARH + EVI	554.16	1.67	0.172	< 0.001*	58.96	12.48	0.524	0.026*
MAT + MARH + $\delta^{18}O_{meteoric}$	554.33	1.83	0.204	< 0.001*	54.70	8.22	0.247	0.316
MAT + EVI + $\delta^{18}O_{meteoric}$	566.36	13.87	0.203	< 0.001*	60.16	13.68	0.423	0.077
MAP + MARH + EVI	560.38	7.89	0.127	< 0.001*	52.21	5.73	0.188	0.458
MAP + MARH + $\delta^{18}O_{meteoric}$	562.29	9.79	0.166	< 0.001*	51.98	5.50	0.506	0.032*
MAP + EVI + $\delta^{18}O_{meteoric}$	566.61	14.12	0.154	< 0.001*	47.96	1.49	0.513	0.030*
MARH + EVI + $\delta^{18}O_{meteoric}$	560.44	7.95	0.125	< 0.001*	54.22	7.74	0.621	0.007*
MAT + MAP + MARH + EVI	554.75	2.26	0.165	< 0.001*	50.09	3.61	0.440	0.065
MAT + MAP + MARH + $\delta^{18}O_{meteoric}$	554.67	2.18	0.213	< 0.001*	53.37	6.89	0.618	0.022*
MAT + MAP + EVI + $\delta^{18}O_{meteoric}$	560.19	7.69	0.213	< 0.001*	49.89	3.41	0.531	0.061
MAT + MARH + EVI + $\delta^{18}O_{meteoric}$	555.93	3.43	0.180	< 0.001*	55.59	9.11	0.623	0.021*
MAP + MARH + EVI + $\delta^{18}O_{meteoric}$	562.33	9.84	0.206	< 0.001*	46.48	0.00	0.462	0.117
MAT + MAP + MARH + EVI + $\delta^{18}O_{meteoric}$	556.54	4.04	0.166	< 0.001*	47.42	0.95	0.695	0.007*

Table 1.5: Models predicting stable oxygen isotope values for *Trichosurus vulpecula* and *Trichosurus caninus*. Here, MAT refers to max. MAT. Asterisks indicate significance at $\alpha = 0.05$. The model with the lowest AIC score is highlighted grey, unless $p > 0.05$. If so, the model is outlined in black and the model with the second lowest AIC score highlighted.

	Asfc				*epLsar*			
	AIC	Δ	R^2	*p*	AIC	Δ	R^2	*p*
Latitude	638.97	181.67	0.034	0.020*	-1614.51	0.00	0.018	0.089
MAT	457.30	0.00	0.046	0.021*	-1143.83	470.68	0.003	0.545
MAP	460.25	2.95	0.021	0.120	-1143.60	470.91	0.007	0.367
MARH	462.03	4.73	0.021	0.121	-1143.46	471.05	0.001	0.706
EVI	462.70	5.40	0.006	0.416	-1143.84	470.66	< 0.001*	0.937
MAT + MAP	458.07	0.77	< 0.001*	0.936	-1141.89	472.62	0.003	0.537
MAT + MARH	459.19	1.89	0.057	0.040*	-1141.88	472.63	0.004	0.808
MAT + EVI	459.25	1.95	0.047	0.068	-1142.13	472.38	0.004	0.814
MAP + MARH	458.02	0.72	0.047	0.070	-1141.62	472.88	0.006	0.719
MAP + EVI	461.80	4.50	0.057	0.039*	-1142.25	472.26	0.001	0.920
MARH + EVI	463.98	6.68	0.025	0.243	-1141.95	472.56	0.007	0.678
MAT + MAP + MARH	458.28	0.98	0.006	0.702	-1139.90	474.61	0.004	0.786
MAT + MAP + EVI	460.02	2.72	0.071	0.043*	-1140.39	474.12	0.004	0.934
MAT + MARH + EVI	461.06	3.76	0.057	0.090	-1140.32	474.19	0.008	0.824
MAP + MARH + EVI	459.95	2.66	0.048	0.140	-1140.25	474.26	0.008	0.840
MAT + MAP + MARH + EVI	460.28	2.98	0.058	0.088	-1138.42	476.09	0.007	0.856

Table 1.6: Models predicting DMTA values for all *Trichosurus*. All environmental variables have been matched to the month of specimen collection. Here, MAT refers to max. MAT. Asterisks indicate significance at $\alpha = 0.05$. The model with the lowest AIC score is highlighted grey, unless $p > 0.05$. If so, the model is outlined in black and the model with the second lowest AIC score highlighted.

BIBLIOGRAPHY

Arman, S.D., Ungar, P.S., Brown, C.A., DeSantis, L.R.G., Schmidt, C., & Prideaux, G.J. (2016) Minimizing inter–microscope variability in dental microwear texture analysis. *Surface Topography: Metrology and Properties*, 4.

Auguie, B. (2017). gridExtra: Miscellaneous Functions for "Grid" Graphics. R package version 2.3. https://CRAN.R-project.org/package=gridExtra

Bergmann, C. (1848) *´Uber die Verh´altnisse der W´arme´okonomie der Thiere zu ihrer Gr´osse.*

Bivand, R., Keitt, T., and Rowlingson, B. (2018). rgdal: Bindings for the 'Geospatial' Data Abstraction Library. R package version 1.2-18. https://CRAN.R-project.org/package=rgdal.

Bivand, R. and Lewin-Koh, N. (2017). maptools: Tools for Reading and Handling Spatial Objects. R package version 0.9-2. https://CRAN.R-project.org/package=maptools

Black, K.H., Archer, M., Hand, S.J., & Godthelp, H. (2012) The Rise of Australian Marsupials: A Synopsis of Biostratigraphic, Phylogenetic, Palaeoecologic and Palaeobiogeographic Understanding. *Earth and Life* (ed. by J.A. Talent), pp. 983—1078. Springer Netherlands, Dordrecht.

Black, K.H., Price, G.J., Archer, M., & Hand, S.J. (2014) Bearing up well? Understanding the past, present and future of Australias koalas. *Gondwana Research* 25, 1186—1201.

Bowen, G. J. (2018) The Online Isotopes in Precipitation Calculator, version 3.1. http://www.waterisotopes.org.

Bowen, G.J. & Revenaugh, J. (2003) Interpolating the isotopic composition of modern meteoric precipitation: isotopic composition of modern precipitation. *Water Resources Research*, 39.

Bowen, G.J., Wassenaar, L.I., & Hobson, K.A. (2005) Global application of stable hydrogen and oxygen isotopes to wildlife forensics. *Oecologia*, 143, 337—348.

Brookman, T.H. & Ambrose, S.H. (2012) Seasonal variation in kangaroo tooth enamel oxygen and carbon isotopes in southern Australia. *Quaternary Research*, 78, 256—265.

Burbidge, A., Johnson, K., Fuller, P., & Southgate, R. (1988) Aboriginal Knowledge of the Mammals of the Central Deserts of Australia. *Wildlife Research*, 15, 9.

Burgman, J.H.E., Leichliter, J., Avenant, N.L., & Ungar, P.S. (2016) Dental microwear of sympatric rodent species sampled across habitats in southern Africa: Implications for environmental influence. *Integrative Zoology*, 11, 111—127.

Cerling, T.E., Harris, J.M., MacFadden, B.J., Leakey, M.G., Quade, J., Eisenmann, V., & Ehleringer, J.R. (1997) Global vegetation change through the Miocene/Pliocene boundary. *Nature*, 389, 153—158.

Cerling, T.E., Hart, J.A., & Hart, T.B. (2004) Stable isotope ecology in the Ituri Forest. *Oecologia*, 138, 5—12.

Cernusak, L.A., Tcherkez, G., Keitel, C., Cornwell, W.K., Santiago, L.S., Knohl, A., Barbour, M.M., Williams, D.G., Reich, P.B., Ellsworth, D.S., Dawson, T.E., Griffiths, H.G.,

Farquhar, G.D., & Wright, I.J. (2009) Why are non–photosynthetic tissues generally ^{13}C enriched compared with leaves in C_3 plants? Review and synthesis of current hypotheses. *Functional Plant Biology*, 36, 199.

Cleugh, H., Battaglia, M., Graham, P., & Smith, M.S. (2011) *Climate Change: Science and Solutions for Australia.* CSIRO Publishing, Clayton.

Clout, M.N. & Efford, M.G. (1984) Sex Differences in the Dispersal and Settlement of Brushtail Possums (*Trichosurus vulpecula*). *The Journal of Animal Ecology*, 53, 737.

Coplen, T.B. (1995) Reporting of stable hydrogen, carbon, and oxygen isotopic abundances. *Geothermics*, 24, 707—712.

Cruz, J., Sutherland, D.R., Martin, G.R., & Leung, L.K.–P. (2012) Are smaller subspecies of common brushtail possums more omnivorous than larger ones? Diet and body size in common brushtail possums. *Austral Ecology*, 37, 893—902.

DeGabriel, J.L., Moore, B.D., Foley, W.J., & Johnson, C.N. (2009) The effects of plant defensive chemistry on nutrient availability predict reproductive success in a mammal. *Ecology*, 90, 711—719.

Demment, M.W. & Van Soest, P.J. (1985) A nutritional explanation for body-size patterns of ruminant and nonruminant herbivores. *American Naturalist*, 125, 641—72.

DeSantis, L.R.G. (2016) Dental microwear textures: reconstructing diets of fossil mammals. *Surface Topography: Metrology and Properties*, 4.

DeSantis, L.R.G., Feranec, R.S., MacFadden, B.J. (2009) Effects of Global Warming on Ancient Mammalian Communities and Their Environments. *PLoS ONE* 4.

DeSantis, L.R.G., Field, J.H., Wroe, S., & Dodson, J.R. (2017) Dietary responses of Sahul (Pleistocene Australia—New Guinea) megafauna to climate and environmental change. *Paleobiology*—15.

DeSantis, L.R.G. & Hedberg, C. (2017) Stable isotope ecology of the koala (Phascolarctos cinereus). *Australian Journal of Zoology*, 64, 353.

Didan, K. (2015) MOD13C2 MODIS/Terra Vegetation Indices Monthly L3 Global 0.05Deg CMG V006.

Evans, M. (1992) Diet of the Brushtail Possum *Trichosurus vulpecula* (Marsupialia: Phalangeridae) in central Australia. *Australian Mammalogy*, 15, 25—30.

Farquhar, G.D. & Lloyd, J. (1993) Carbon and Oxygen Isotope Effects in the Exchange of Carbon Dioxide between Terrestrial Plants and the Atmosphere. *Stable Isotopes and Plant Carbon–water Relations* pp. 47—70. Elsevier.

Fischer, J., Lindenmayer, D.B., Nix, H.A., Stein, J.L., & Stein, J.A. (2001) Climate and animal distribution: a climatic analysis of the Australian marsupial *Trichosurus caninus*. *Journal of Biogeography*, 28, 293—304.

Fitzgerald, A.E., Smith, A., & Hume, I. (1984) Diet of the possum (*Trichosurus vulpecula*) in three Tasmanian forest types and its relevance to the diet of possums in New Zealand forests. *Possums and Gliders* pp. 137—143. Australian Mammal Society, Sydney.

Fraser, R.A. *A study of stable carbon, nitrogen and oxygen isotopes in modern Australian marsupial herbivores, and their relationships with environmental conditions*. Australia National University, Canberra, Australia.

Fraser, R.A., Gr$\acute{}$un, R., Privat, K., & Gagan, M.K. (2008) Stable–isotope microprofiling of wombat tooth enamel records seasonal changes in vegetation and environmental conditions in eastern Australia. *Palaeogeography, Palaeoclimatology, Palaeoecology*, 269, 66—77.

Freeland, W.J. & Winter, J.W. (1976) Evolutionary consequences of eating: *Trichosurus vulpecula* (marsupialia) and the genus *Eucalyptus*. *Journal of Chemical Ecology*, 1, 439—455.

Friedman, I. & ONeil, J.R. (1977) *Data of Geochemistry: Compilation of stable isotope fractionation factors of geochemical interest*. U.S. Government Printing Office.

Fulton, G.R. (2017) Native marsupials as egg predators of artificial ground–nests in Australian woodland. *Australian Journal of Zoology*, 65, 196.

Glenn, E.P., Huete, A.R., Nagler, P.L., & Nelson, S.G. (2008) Relationship between remotely–sensed vegetation indices, canopy attributes and plant physiological processes: What vegetation indices can and cannot tell us about the landscape. *Sensors*, 8, 2136—2160.

Gloury, A.M. & Handasyde, K.A. (2016) Comparative dietary ecology of two congeneric marsupial folivores. *Austral Ecology*, 41, 355—366.

Grine, F.E. (1986) Dental evidence for dietary differences in Australopithecus and Paranthropus: a quantitative analysis of permanent molar microwear. *Journal of Human Evolution*, 15, 783—822.

Harrell, F. E. (2018). Hmisc: Harrell Miscellaneous. R package version 4.1–1. https://CRAN.R-project.org/package=Hmisc.

Hedberg, C. & DeSantis, L.R.G. (2017) Dental microwear texture analysis of extant koalas: clarifying causal agents of microwear. *Journal of Zoology*, 301, 206—214.

Hijmans, R. J. (2017). raster: Geographic Data Analysis and Modeling. R package version 2.6-7. https://CRAN.R-project.org/package=raster.

Hocknull, S.A., Zhao, J., Feng, Y., & Webb, G.E. (2007) Responses of Quaternary rainforest vertebrates to climate change in Australia. *Earth and Planetary Science Letters*, 264, 317—331.

How, A. (1978) Population Strategies of four species of Australian possums. *The ecology of arboreal folivores* pp. 305—313. Smithsonian Institution Press, Washington.

How, R.A. & Hillcox, S.J. (2000) Brushtail possum, *Trichosurus vulpecula*, populations in south–western Australia: demography, diet and conservation status. *Wildlife Research*, 27, 81—89.

IAEA/WMO (2015). Global Network of Isotopes in Precipitation. The GNIP Database. Accessible at: https://nucleus.iaea.org/wiser.

Janis, C.M., Damuth, J., & Theodor, J.M. (2000) Miocene ungulates and terrestrial primary productivity: Where have all the browsers gone? *Proceedings of the National Academy of Sciences*, 97, 7899—7904.

Johnson, K.A., McQuillan, P.B., & Kirkpatrick, J.B. (2011) Nocturnal Mammals, Diurnal Lizards, and the Pollination Ecology of the Cryptic Flowering *Acrotriche Serrulata* (Ericaceae). I*nternational Journal of Plant Sciences*, 172, 173—182.

Jones, B.D. & DeSantis, L.R.G. (2017) Dietary ecology of ungulates from the La Brea tar pits in southern California: a multi-proxy approach. *Palaeogeography, Palaeoclimatology, Palaeoecology* 466: 110127

Jouzel, J., Masson–Delmotte, V., Cattani, O., Dreyfus, G., Falourd, S., Hoffman, G., Minster, B., Nouet, J., Barnola, J. M., Chappellaz, J., Fischer, H., Gallet, J. C., Johnsen, S., Leuenberger, M. Loulergue, L., Luethi, D., Oerter, H., Parrenin, F., Raisbeck, G., Raynaud, D., Schilt, A., Schwander, J., Selmo, E., Souchez, R., Spahni, R., Stauffer, B., Steffensen, J. P., Stenni, B., Stocker, T. F., Tison, J. L., Werner, M., Wolff, E. W. (2007) Orbital and Millennial Antarctic Climate Variability over the Past 800,000 Years. *Science*, 317, 793—796.

Kerle, A. (2001) *Possums: the brushtails, ringtails, and greater glider*. UNSW Press, Sydney.

Kerle, J.A. (1984) Variation in the ecology of *Trichosurus*: its adaptive significance. *Possums and Gliders* pp. 115—128. Australian Mammal Society,

Kerle, J.A. (1985) Habitat preference and diet of the northern brushtail possum *Trichosurus arnhemensis* in the Alligator Rivers Region, N. T. *Proceedings of the Ecological*

Society of Australia, 13, 161—176.

Kerle, J.A. (1998) The population dynamics of a tropical possum, *Trichosurus vulpecula arnhemensis* Collett. *Wildlife Research*, 25, 171.

Kerle, J. A. & Burgman, M. (1984) Some Aspects of the Ecology of the Mammal Fauna of the Jabiluka Area. Northern Territory. *Wildlife Research*, 11, 207.

Kerle, J.A., McKay, G.M., & Sharman, G.B. (1991) A systematic analysis of brushtail possum, *Trichosurus vulpecula* (Kerr, 1792) (Marsupialia: Phalangxeridae). *Australian Journal of Zoology*, 39, 313—331.

Kershaw, P., Moss, P., & Van Der Kaars, S. (2003) Causes and consequences of long–term climatic variability on the Australian continent. *Freshwater Biology*, 48, 1274—1283.

Laurance, W.F., Laurance, S.G., & Hilbert, D.W. (2008) Long–Term Dynamics of a Fragmented Rainforest Mammal Assemblage. *Conservation Biology*, 22, 1154—1164.

Levin, N.E., Cerling, T.E., Passey, B.H., Harris, J.M., & Ehleringer, J.R. (2006) A stable isotope aridity index for terrestrial environments. *Proceedings of the National Academy of Sciences*, 103, 11201—11205.

Macfadden, B.J., Cerling, T.E., Harris, J.M., & Prado, J. (1999) Ancient latitudinal gradients of C_3/C_4 grasses interpreted from stable isotopes of New World Pleistocene horse (Equus) teeth. *Global Ecology and Biogeography*, 8, 137—149.

Maclean, I.M.D. & Wilson, R.J. (2011) Recent ecological responses to climate change

support predictions of high extinction risk. *Proceedings of the National Academy of Sciences*, 108, 12337—12342.

Martin, R. & Handasyde, K.A. (1999) *The koala: natural history, conservation and management*. Krieger Pub. Co., Malabar, Fla.

Merceron, G., Ramdarshan, A., Blondel, C., Boisserie, J.–R., Brunetiere, N., Francisco, A., Gautier, D., Milhet, X., Novello, A., & Pret, D. (2016) Untangling the environmental from the dietary: dust does not matter. *Proceedings of the Royal Society B: Biological Sciences*, 283, 20161032.

Molloy, S.W. & Davis, R.A. (2017) Resilience to agricultural habitat fragmentation in an arboreal marsupial. *Australian Mammalogy*, 39, 185.

Molloy, S.W., Davis, R.A., & van Etten, E.J.B. (2016) Incorporating Field Studies into Species Distribution and Climate Change Modelling: A Case Study of the Koomal *Trichosurus vulpecula hypoleucus* (Phalangeridae). *PLOS ONE*, 11.

Morgan, M.E., Kingston, J.D., & Marino, B.D. (1994) Carbon isotopic evidence for the emergence of C_4 plants in the Neogene from Pakistan and Kenya. *Nature*, 367, 162—165.

Munks, S.A., Corkrey, R., & Foley, W.J. (1996) Characteristics of arboreal marsupial habitat in the semi–arid woodlands of northern Queensland. *Wildlife Research*, 23, 185—195.

Murphy, B.P., Bowman, D.M., & Gagan, M.K. (2007a) The interactive effect of temperature and humidity on the oxygen isotope composition of kangaroos. *Functional Ecology*,

21, 757—766.

Murphy, B.P., Bowman, D.M. and Gagan, M.K., (2007b) Sources of carbon isotope variation in kangaroo bone collagen and tooth enamel. *Geochimica et Cosmochimica Acta*, 71.

Murphy, B.P. & Davies, H.F. (2014) There is a critical weight range for Australias declining tropical mammals. *Global ecology and biogeography*, 23, 1058—1061.

Owen, W.H. & Thomson, J.A. (1965) Notes of the comparative ecology of the common brushtail and mountain possums in eastern Australia. *Victorian Naturalist*, 82, 216—217.

Prideaux, G.J., Ayliffe, L.K., DeSantis, L.R.G., Schubert, B.W., Murray, P.F., Gagan, M.K., & Cerling, T.E. (2009) Extinction implications of a chenopod browse diet for a giant Pleistocene kangaroo. *Proceedings of the National Academy of Sciences*, 106, 11646—11650.

Prideaux, G.J., Long, J.A., Ayliffe, L.K., Hellstrom, J.C., Pillans, B., Boles, W.E., Hutchinson, M.N., Roberts, R.G., Cupper, M.L., Arnold, L.J., Devine, P.D., & Warburton, N.M. (2007) An arid–adapted middle Pleistocene vertebrate fauna from south–central Australia. *Nature*, 445, 422—425.

Proctor–Grey, E. (1984) Dietary ecology of the coppery brushtail possum, green ringtail possum and Lumholtzs tree kangaroo in north Queensland. *Possums and Gliders* (ed. by A. Smith and I. Hume), pp. 129—135. Australian Mammal Society.

Revelle, W. (2018) psych: Procedures for Personality and Psychological Research, Northwestern University, Evanston, Illinois, USA, https://CRAN.R-project.org/package=psych

Version = 1.8.4.

Roberts, P., Blumenthal, S.A., Dittus, W., Wedage, O., & Lee–Thorp, J.A. (2017) Stable carbon, oxygen, and nitrogen, isotope analysis of plants from a South Asian tropical forest: Implications for primatology. *American Journal of Primatology*, 79,

Schulz, E., Piotrowski, V., Clauss, M., Mau, M., Merceron, G., & Kaiser, T.M. (2013) Dietary Abrasiveness Is Associated with Variability of Microwear and Dental Surface Texture in Rabbits. *PLoS ONE*, 8.

Scott, R.S., Teaford, M.F., & Ungar, P.S. (2012) Dental microwear texture and anthropoid diets. *American Journal of Physical Anthropology*, 147, 551—579.

Scott, R.S., Ungar, P.S., Bergstrom, T.S., Brown, C.A., Childs, B.E., Teaford, M.F., & Walker, A. (2006) Dental microwear texture analysis: technical considerations. *Journal of Human Evolution*, 51, 339—349.

Scott, R.S., Ungar, P.S., Bergstrom, T.S., Brown, C.A., Grine, F.E., Teaford, M.F., & Walker, A. (2005) Dental microwear texture analysis shows within–species diet variability in fossil hominins. *Nature*, 436, 693—695.

Secord, R., Bloch, J.I., Chester, S.G.B., Boyer, D.M., Wood, A.R., Wing, S.L., Kraus, M.J., McInerney, F.A., & Krigbaum, J. (2012) Evolution of the Earliest Horses Driven by Climate Change in the Paleocene–Eocene Thermal Maximum. *Science*, 335, 959—962.

Sims, D., Luo, H., Hastings, S., Oechel, W., Rahman, A., & Gamon, J. (2006) Parallel adjustments in vegetation greenness and ecosystem CO2 exchange in response to

drought in a Southern California chaparral ecosystem. *Remote Sensing of Environment*, 103, 289—303.

Smiley, T.M., Cotton, J.M., Badgley, C., & Cerling, T.E. (2016) Small–mammal isotope ecology tracks climate and vegetation gradients across western North America. *Oikos*, 125, 1100—1109.

Statham, H.L. (1984) The diet of *Trichosurus vulpecula* (Kerr) in four Tasmanian forest locations. *Possums and Gliders* (ed. by A. Smith and I. Hume) pp. 213—219. Australian Mammal Society,

Travouillon, K.J., Legendre, S., Archer, M., & Hand, S.J. (2009) Palaeoecological analyses of Riversleighs Oligo–Miocene sites: Implications for Oligo–Miocene climate change in Australia. *Palaeogeography, Palaeoclimatology, Palaeoecology*, 276, 24—37.

Ungar, P.S., Brown, C.A., Bergstrom, T.S., & Walkers, A. (2003) Quantification of dental microwear by tandem scanning confocal microscopy and scale–sensitive fractal analyses. *Scanning*, 25, 185—193.

Ungar, P.S., Grine, F.E., & Teaford, M.F. (2008) Dental Microwear and Diet of the Plio–Pleistocene Hominin Paranthropus boisei. *PLoS ONE*, 3, e2044.

van der Merwe, N.J. & Medina, E. (1989) Photosynthesis and ratios in Amazonian rain forests. *Geochimica et Cosmochimica Acta*, 53, 1091—1094.

van der Merwe, N.J. & Medina, E. (1991) The canopy effect, carbon isotope ratios and foodwebs in Amazonia. *Journal of Archaeological Science*, 18, 249—259.

Wickham, H. (2009). ggplot2: Elegant Graphics for Data Analysis. Springer–Verlag New York.

Wickham, H., Francois, R., Henry, L. and Mller, K. (2017). dplyr: A Grammar of Data Manipulation. R package version 0.7.4. https://CRAN.R-project.org/package=dplyr

Williams, S.E., Bolitho, E.E., & Fox, S. (2003) Climate change in Australian tropical rainforests: an impending environmental catastrophe. *Proceedings of the Royal Society B: Biological Sciences*, 270, 1887—1892.

Woinarski, J., Burbidge, A., & Harrison, P. (2015) Ongoing unraveling of a continental fauna: Decline and extinction of Australian mammals since European settlement. *Proceedings of the National Academy of Sciences* 112, 4531—4540.

Xia, J., Zheng, J., Huang, D., Tian, Z.R., Chen, L., Zhou, Z., Ungar, P.S., & Qian, L. (2015) New model to explain tooth wear with implications for microwear formation and diet reconstruction. *Proceedings of the National Academy of Sciences*, 112, 10669—10672.

Yom–Tov, Y., Green, W.O., & Coleman, J.D. (2009) Morphological trends in the Common brushtail possum, *Trichosurus vulpecula*, in New Zealand. *Journal of Zoology*, 208, 583—593.